Available online at www.sciencedirect.com
ScienceDirect
Catalysis Today 128 (2007) 168–175
CATALYSIS TODAY
www.elsevier.com/locate/cattod

Parameters influencing the synergetic effect induced by vanadium incorporation on non-conventional (Al)(Ga)PO supports for the propane ammoxidation

M.A. Soria *, P. Ruiz, E.M. Gaigneaux

Unité de catalyse et chimie des matériaux divisés, Université catholique de Louvain, Croix du Sud 2/17, 1348 Louvain-la-Neuve, Belgium

Available online 21 September 2007

Abstract

A series of V-oxide supported catalysts ($5V/AlPO_4$, $5V/Al_{0.5}Ga_{0.5}PO_4$, $5V/GaPO_4$) were prepared in order to study their catalytic behaviour in the ammoxidation of propane. Catalysts were characterized by BET surface area, XRD, Raman spectroscopy, TPR-H_2 and XPS. The presence of vanadium induced the crystallization of the supports ($AlPO_4$, $Al_{0.5}Ga_{0.5}PO_4$ and $GaPO_4$). Crystalline V_2O_5 was observed on the V-based catalysts. Catalytic results showed that the impregnation of vanadium enhances the propane conversion and selectivity to acrylonitrile (ACN). At 530 °C $5V/Al_{0.5}Ga_{0.5}PO_4$ exhibits the highest selectivity to ACN. One assumes that the best performance of $5V/Al_{0.5}Ga_{0.5}PO_4$ in propane ammoxidation, is due to on the one hand the easiest reduction of V_2O_5 on $Al_{0.5}Ga_{0.5}PO_4$ and to on the other hand a certain tunability of the reduced species stabilized on $Al_{0.5}Ga_{0.5}PO_4$.

Keywords: Acrylonitrile; Ammoxiadtion of propane; Vanadium oxide; Aluminophosphate; Galloaluminophosphate; Gallophosphate

1. Introduction

Currently acrylonitrile is commercially produced mainly by ammoxidation of propylene, but new developments have indicated the possibility of selective one-stage synthesis of acrylonitrile, from propane. Selective ammoxidation of propane into acrylonitrile is an attractive alternative process, as (i) acrylonitrile is widely used in the petrochemical industry, (ii) propane is abundant and its cost is about 50% lower than that of propylene [1,2] and (iii) there is a risk of propylene shortage due to its increasing demand in the petrochemical industry. Thus the development of a process based on propane as the starting molecule appears to be the most direct evolution of the propylene ammoxidation:

$$CH_3{-}CH_2{-}CH_3 + NH_3 + 2O_2 \Rightarrow CH_2{=}CH{=}CN + 4H_2O$$
$$(\Delta H = -632\,\mathrm{kJ/mol})$$

Many catalysts have been tested using oxides containing vanadium as a key component, e.g., modified V–Sb oxides [2,3] Mo–V–Te–Nb oxides [4,5], $(VO)_2P_2O_7$ [6,7] and V–Al oxynitrides [8,9].

We recently [10] evidenced the possibility to dramatically boost the selectivity of a $Al_{0.5}Ga_{0.5}PO_4$ catalyst in the ammoxidation of propane by supporting V oxide on it. In continuation, the objective of this work is to further elucidate the mechanism of such synergy by identifying the parameters dictating its extent. Therefore, we investigated the behaviour of a set of catalysts made of V oxide supported on three supports differing by their composition ($AlPO_4$, $Al_{0.5}Ga_{0.5}PO_4$ and $GaPO_4$) and thus by their acidity. Acidity of the support may indeed be a parameter influencing the synergy with vanadium oxide. This approach will also eventually allow to indirectly tuning the reducibility of the vanadium phases, which could be another factor to investigate.

2. Experimental

2.1. Catalyst preparation

The supports were prepared by using the process developed by Kearby [11] for aluminophosphates ($AlPO_4$) and adapted for the $Al_{0.5}Ga_{0.5}PO_4$ and $GaPO_4$. The method used for the

* Corresponding author. Tel.: +32 10473590; fax: +32 10473649.
E-mail address: soria@cata.ucl.ac.be (M.A. Soria).

0920-5861/$ – see front matter © 2007 Elsevier B.V. All rights reserved.
doi:10.1016/j.cattod.2007.06.083

preparation of $Al_{0.5}Ga_{0.5}PO_4$ was detailed previously in [10]. Starting material was a solution of adequate amounts of $Ga(NO_3)_3{\cdot}5H_2O$, $AlCl_3$ and H_3PO_4 2 M (Ga/P atomic ratio of 1). The other supports were prepared following the same procedure as for $Al_{0.5}Ga_{0.5}PO_4$, but using different starting products, namely: (i) for $AlPO_4$ a solution of adequate amounts of $AlCl_3$ and H_3PO_4 2 M (Al/P atomic ratio of 1), and (ii) for $GaPO_4$ a solution of adequate amounts of $Ga(NO_3)_3{\cdot}5H_2O$ and H_3PO_4 2 M (Ga/P atomic ratios of 1). The resulting powders were calcined in air at 800 °C ($AlPO_4$), 650 °C ($Al_{0.5}Ga_{0.5}PO_4$) and at 625 °C ($GaPO_4$) during 3 h. As already shown in a previous work [12], the $Al_{0.5}Ga_{0.5}PO_4$ obtained was truly a single phase, although amorphous, but not a mixture of $AlPO_4$ and $GaPO_4$.

The vanadium containing catalysts (5% wt. of V) were prepared by wet impregnation of $AlPO_4$, $Al_{0.5}Ga_{0.5}PO_4$, and $GaPO_4$ with an aqueous solution of NH_4VO_3 (0.03 M), which was prepared by heating at 60 °C under stirring, and with the pH adjusted to 5.5 by adding ammonium hydroxide (10%, v/v). The solvent was evaporated in a rotavapor, then dried at 110 °C for 16 h and calcined at 500 °C for 3 h in air. Samples referred to as $5V/AlPO_4$, $5V/Al_{0.5}Ga_{0.5}PO_4$, and $5V/GaPO_4$. As a first reference sample, a silica (Degussa, 41 m^2/g) was impregnated with 5% wt. of V using the same impregnation solution as for the phosphate materials and following the same procedure. The obtained sample is denoted $5V/SiO_2$.

Another series of reference samples consists in three mechanical mixtures of V_2O_5 and $AlPO_4$ (referred to as MM_1), V_2O_5 and $Al_{0.5}Ga_{0.5}PO_4$ (referred to as MM_2) and V_2O_5 and $GaPO_4$ (referred to as MM_3). Each mixture contains 5% wt. of V and was prepared following the procedure detailed in [10].

2.2. Characterization

2.2.1. Textural properties

Textural analysis was carried out in a Micromeritics Tristar 3000 equipment using the adsorption of nitrogen at −196 °C, working with relative P/P_0 pressures in the range of 10^{-2} to 1.0. For each analysis, 150 mg of sample were degassed under vacuum (50 mTorr) at 150 °C. The specific surface area was thus calculated from the quantity of gas adsorbed (theory of Brunauer, Emmet and Teller [13] by using 5 points with relative P/P_0 pressures ranging between 5×10^{-2} and 0.3. The distribution of pores diameter was determined by the BJH method (Barret, Joiyner and Halenda [14]) and the total pore volume was assessed from the amount of nitrogen adsorbed at a relative pressure of about 0.98.

2.2.2. X-ray diffraction (XRD)

XRD was recorded on a Siemens D5000 diffractometer using the Kα radiation of Cu (λ = 1.5418 Å). The 2θ range between 5° and 70° was scanned at a rate of 0.02 °/s. For XRD in situ, the apparatus was equipped with a high temperature chamber HTK10 from Anton Paar., provided with a furnace allowing the control of the atmosphere and the programming of temperature. A first X-ray diffraction pattern of the sample not calcined was recorded at room temperature, then the sample was heated until 500 °C under air with a rise in temperature of 5 °C/min. Three XRD patterns were recorded with 1 h intervals when the temperature reached 500 °C. The 2θ range between 5° and 37° was scanned, at a rate of 0.02°/s, in order to allow a focusing on the area where the most intense peaks of crystalline V_2O_5 and crystalline phases of the supports appear.

2.2.3. Ammonia chemisorption

Ammonia chemisorption was conducted on 100 mg of catalyst at 35 °C using the static volumetric apparatus Micromeritics ASAP 2010C adsorption analyzer. The samples were previously heated 3 h at 350 °C a flow of 30 ml/min of He. In order to differentiate between ammonia physisorption and chemisorption, the analysis was repeated after the first isotherm. A first isotherm allows evaluating the volumes of ammonia physisorbed and chemisorbed at different pressures. After evacuation of the physisorbed fraction at the analysis temperature for 0.5 h, a second isotherm is used to determine the fraction reversibly adsorbed. The volume of ammonia chemisorbed is estimated by subtraction between those two isotherms. In this work, only the ammonia chemisorption results are presented. Reproducibility is of about 10%.

2.2.4. Raman spectroscopy

Raman spectroscopy was performed with a Dilor-Jobin Yvon-Spex spectrometer model Labram interfaced with an optical microscope OLYMPUS DX-40, and equipped with a He–Ne (λ = 632.8 nm) laser. Spectra were obtained by averaging 3 scans of the Raman shift range between 200 and 1200 cm^{-1}, each of them recorded in 30 s with a spectral resolution of 7 cm^{-1}.

2.2.5. H_2 temperature programmed reduction (TPR)

TPR was carried out in a continuous flow fixed bed reactor operating at atmospheric pressure. One hundred milligrams of sample were placed in a vertical reactor made of quartz. The sample was pre-treated by heating it in a He gas flow (50 ml/min) to 400 °C and then maintaining this temperature for 2 h. After cooling, the sample was tested by increasing the temperature from 40 to 850 °C. The reducing gas, a mixture of 5 vol.% H_2 in He at a flow rate of 50 ml min^{-1}, was used to reduce the catalyst with a continuous temperature ramp (10 °C/min). The inlet and outlet gas compositions were measured using a QMC 311 Balzers quadrupole mass spectrometer coupled to the reactor.

2.2.6. XPS

XPS analyses were performed on an Axis Ultra spectrometer from Kratos working with a non-monochromatic Mg radiation (10 mA, 15 kV) and the charge compensation device provided by the supplier (charge balance fixed at −2.3 V). The samples powders were pressed in small stainless steel troughs mounted on a multi specimen holder. The pressure in the analysis chamber was around 10^{-6} Pa. The angle between the normal of the sample surface and the lens axis was 0°. The hybrid lens magnification mode was used with the slot aperture resulting in an analyzed area of 700 μm × 300 μm. The pass energy for the

analyzer was 40 eV. In these conditions, the energy resolution gives a full width at half maximum (FWHM) of the Ag $3d_{5/2}$ peak of about 1 eV. The following sequence of spectra was recorded: survey spectrum, C_{1s}, O_{1s} & V_{2p}, Al_{2p}, Ga_{3d} and O_{2s} Ga_{3p} and C_{1s} again to check the stability of charge compensation in function of time and the absence of degradation of the sample during the analyses. The binding energies were calibrated by fixing the C–(C, H) contribution of the C1s adventitious carbon at 284.8 eV. Peaks were considered to be combinations of Gaussian and Lorentzian functions in a 70/30 ratio working with linear baseline (following recommendations from the supplier). For the quantification of the elements, sensibility factors provided by the manufacturer were used. Data treatment was performed with the CasaXPS program (Casa Software Ltd., UK). XPS was performed on the fresh samples as well as those after TPR-H_2.

2.3. Catalytic activity

ropane ammoxidation was performed at 500, 530 and 550 °C using a conventional fixed bed quartz microreactor at atmospheric pressure. About 0.1 g catalyst was located in the outlet section of the reactor placed vertically inside on electrical furnace, surrounding the reactor tube. The gas feed consists of a mixture of C_3H_8:O_2:NH_3 in 1.25:3:1 volume ratio. Total flow was 28 ml/min. Feed and products were analysed on-line by two gas chromatographs, equipped with FID and TCD, respectively. A carbon mass balance of 80–90% was obtained, which is likely attributed to: (i) coke deposition (that will be reported in XPS result) and (ii) condensation or the polymerization of acrylonitrile. Although the connection between the reactor and the chromatograph was heated to 150 °C the mass balance observed evidenced that these problems cannot be fully resolved (increasing the temperature is favourable for avoiding condensation but is possibly detrimental for the polymerization aspect). Dead volumes were reduced using quartz grain to diminish contribution from homogeneous conversion. Under these conditions homogenous conversion (i.e. without any support or catalyst in the reactor) was estimated to 8% at 500 °C, 12% at 530 °C and 12% at 550 °C with the main products being propylene and CO_x.

3. Results

3.1. Catalysts characterization

The acidity, the BET surface area (S_{BET}), total pore volume (V_p), and average pore diameter (d_{p_i}) and the XRD phase composition of the metallophosphate supports ($AlPO_4$, $Al_{0.5}Ga_{0.5}PO_4$, $GaPO_4$), silica (SiO_2) and the V-based catalysts ($5V/AlPO_4$, $5V/Al_{0.5}Ga_{0.5}PO_4$, $5V/GaPO_4$, $5V/SiO_2$) are given in Table 1. The $AlPO_4$, $Al_{0.5}Ga_{0.5}PO_4$, $GaPO_4$ supports as well as the V oxide supported catalysts presents a type IV isotherm, according to the IUPAC classification [13]. The supports display a monomodal pores size distribution, whose average pore diameter is labelled as "d_{p_1}" (Table 1). When these supports were impregnated with vanadium, besides the pores of the support (d_{p_1}) larger pores centred at d_{p_2} (see Table 1) were observed, exhibiting a bimodal pore size distribution. For $5V/AlPO_4$ it can be stated that the size of pores of the $AlPO_4$ support increased from 54 (pure support) to 74 Å (denoted as "d_{p_1}", in Table 1), whereas the newly observed larger ones have an average diameter of 180 Å (denoted as "d_{p_2}" in Table 1). Concerning $5V/Al_{0.5}Ga_{0.5}PO_4$, the average diameter of pores of the $Al_{0.5}Ga_{0.5}PO_4$ support, remained constant after vanadium impregnation (30 Å; denoted as "d_{p_1}" in the Table 1) and the newly observed larger pores have an average diameter of 180 Å (denoted as "d_{p_2}" in Table 1). The impregnation of V on $GaPO_4$ resulted in increasing the pores of the support from 50 to 70Å (denoted as "d_{p_1}" in the Tabla1) and the newly observed larger pores have an average value of 280 Å.

The acidity of the supports decreases in the following order: $GaPO_4 > Al_{0.5}Ga_{0.5}PO_4 > AlPO_4 > SiO_2$. After vanadium impregnation, the acidity increases in the case of the $5V/AlPO_4$ and $5V/Al_{0.5}Ga_{0.5}PO_4$ catalysts but it decrease for $5V/GaPO_4$ and $5V/SiO_2$. The acidity of the V-based catalysts decreases as: $5V/Al_{0.5}Ga_{0.5}PO_4 > 5V/GaPO_4 > 5V/AlPO_4 > 5V/SiO_2$.

XRD revealed for the $AlPO_4$, $Al_{0.5}Ga_{0.5}PO_4$ and $GaPO_4$ supports that they remained amorphous during the synthesis

Table 1
Physico-chemical properties of metallophosphates and V-based samples

Sample	Acidity (mmol NH_3/m^2)	S_{BET} (m^2/g)	BJH desorption average pore diameter (Å)		Total pore volume[a] ($cm^3\ g^{-1}$)	XRD phase composition
			d_{p_1}	d_{p_2}[b]		
$AlPO_4$	5.6	345	54	–	0.55	Amorphe
$5V/AlPO_4$	9.8	118	74	180	0.28	V_2O_5 + $AlPO_4$
$Al_{0.5}Ga_{0.5}PO_4$	9.3	288	30	–	0.26	Amorphe
$5V/Al_{0.5}Ga_{0.5}PO_4$	13.5	60	30	180	0.11	V_2O_5 + $Al_{0.5}Ga_{0.5}PO_4$
$GaPO_4$	14.0	125	50	–	0.23	Amorphe
$5V/GaPO_4$	10.9	13	70	280	0.08	V_2O_5 + $GaPO_4$
SiO	5.4	41	133	–	0.08	
$5V/SiO_2$	3.5	36	133	436	0.15	V_2O_5

[a] Total pore volume evaluated from the amount adsorbed at $p/p_0 = 0.98$.
[b] Pore diameter for larger pores, which appeared because of the presence of vanadium.

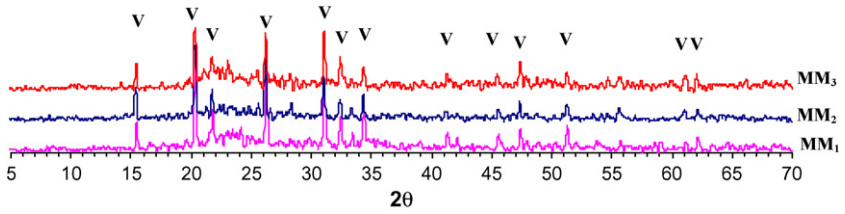

Fig. 1. XRD patterns of V_2O_5 + $AlPO_4$ (MM_1),V_2O_5 + $Al_{0.5}Ga_{0.5}PO_4$ (MM_2) and V_2O_5 + $GaPO_4$ (MM3).

when V is absent. On the contrary, impregnation of vanadium on these supports induced their crystallization. However, the crystallization of the supports is suggested to be partial, because compared to the pure crystalline supports, only the most intense peaks of the support are visible, still as broad bands rather than as sharp peaks. Also, XRD shows the presence of crystalline V_2O_5 in the 5V/$Al_{0.5}Ga_{0.5}PO_4$, 5V/$AlPO_4$, 5V/$GaPO_4$ and 5V/SiO_2 catalysts.

In order to check if this crystalline vanadium oxide is responsible for the crystallization of the supports, three mechanical mixtures: V_2O_5 + $AlPO_4$ (MM_1), V_2O_5 + $Al_{0.5}Ga_{0.5}PO_4$ (MM_2) and V_2O_5 + $GaPO_4$ (MM_3) were prepared. Then, these mechanical mixtures were calcined in the same conditions as for 5V/$AlPO_4$, 5V/ $Al_{0.5}Ga_{0.5}PO_4$ and 5V/$GaPO_4$ catalysts, i.e. at 500 °C during 3 h under air. XRD patterns of these calcined mechanical mixtures MM_1, MM_2 and MM_3 are displayed in Fig. 1. All the diffractograms show peaks characteristic of crystalline V_2O_5 (represented by **V** in Fig. 1). But no peaks of crystalline phases of $AlPO_4$, $Al_{0.5}Ga_{0.5}PO_4$ and $GaPO_4$ are observed in XRD patterns of mechanical mixtures MM_1, MM_2 and MM_3, respectively. Thus one can conclude that: (i) the only presence of crystalline V_2O_5 is not responsible for the crystallisation of the phosphate supports during the 2nd calcination step and (ii) more generally the fact to calcine again at 500 °C does not cause the crystallization of the supports.

In order to carry out an in situ follow-up of the changes of the structure of the solids during calcination, X-ray analyses were realized during a heat treatment in the presence of air. The results of this analysis on the sample 5V/$Al_{0.5}Ga_{0.5}PO_4$ not calcined are shown in Fig. 2, The XRD pattern at room temperature does not present any peaks, demonstrating that one starts from an amorphous sample. However, when the temperature reaches 500 °C, the first diffractogram exhibits three peaks ($2\theta = 21°$, 22°, 36°), which correspond to crystalline $Al_{0.5}Ga_{0.5}PO_4$ support (represented by "S"). The peaks of the crystalline V_2O_5 ($2\theta = 20°$, 26°, 32°, represented by "V") appear in the second XRD pattern. The same was observed for the 5/V $AlPO_4$ and 5V/$GaPO_4$ non-calcined samples (not shown).

The Raman spectra of the V_2O_5, 5V/$Al_{0.5}Ga_{0.5}PO_4$, 5V/$AlPO_4$, 5V/$GaPO_4$ samples in the 250–1200 cm^{-1} region are shown in Fig. 3. Neither the amorphous supports nor the crystalline ones exhibited bands in Raman (not shown). However, the presence of V_2O_5 crystalline in the 5V/$AlPO_4$, 5V/$Al_{0.5}Ga_{0.5}PO_4$, 5V/$GaPO_4$ and 5V/SiO_2 catalysts (bands at 993, 702, 530, 484, 401, 305 and 285 cm^{-1}) is revealed by Raman. The additional presence of polymeric vanadate species was detected in 5V/$AlPO_4$, and 5V/$GaPO_4$ (bands at 930 and 1020 cm^{-1} respectively due to bridging V–O–V bonds and terminal V=O bond) [15,16].

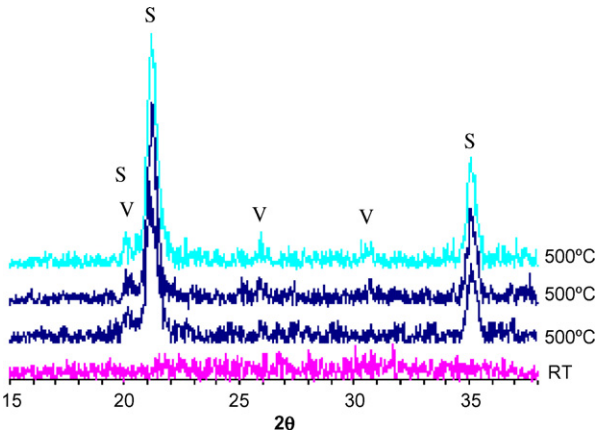

Fig. 2. In situ XRD patterns of the 5V/$Al_{0.5}Ga_{0.5}PO_4$ not calcined.

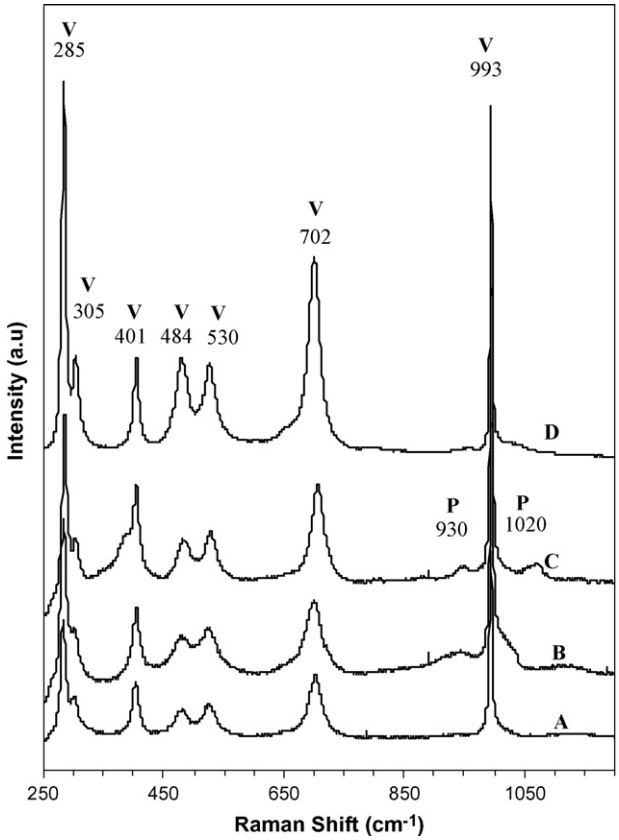

Fig. 3. Raman spectra for (A) 5V/$Al_{0.5}Ga_{0.5}PO_4$, (B)5V/$AlPO_4$ (C) 5V/$GaPO_4$ (D) V_2O_5. (**V**) V_2O_5, (**P**) Polymeric vanadote.

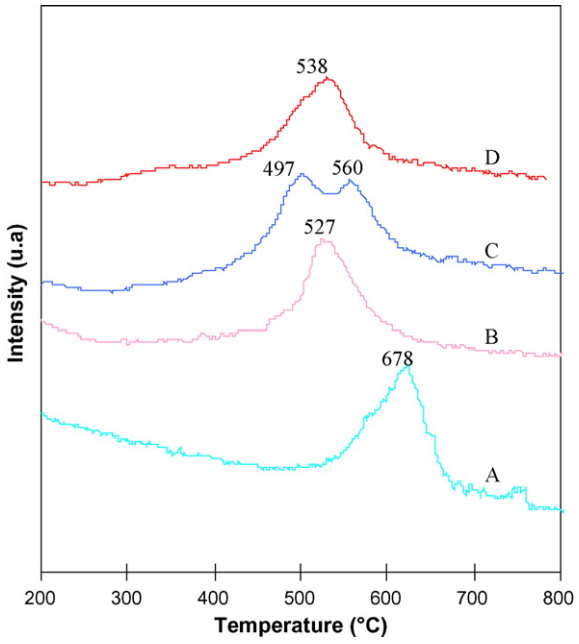

Fig. 4. TPR-H_2 profiles for (A) 5V/SiO_2, (B) 5V/ $AlPO_4$ (C) 5V/$Al_{0.5}Ga_{0.5}PO_4$ and (D) 5V/$GaPO_4$.

Fig. 4 shows the TPR-H_2 profiles for the 5V/$AlPO_4$, 5V/$Al_{0.5}Ga_{0.5}PO_4$, 5V/$GaPO_4$ and 5V/SiO_2 catalysts. The $AlPO_4$, $Al_{0.5}Ga_{0.5}PO_4$ $GaPO_4$ and SiO_2 supports do not present any peak in this technique (not shown). TPR-H_2 profile for 5V/$Al_{0.5}Ga_{0.5}PO_4$ exhibits two major reduction peaks at 497 and 560 °C, whereas 5V/$AlPO_4$, 5V/$GaPO_4$ and 5V/SiO_2 samples present only one major reduction peak at 527, 538 and 678 °C respectively. The TPR-H_2 profile for V_2O_5 exhibits three major reduction peaks at 679, 725 and 900 °C, as described in [10] and confirmed by other authors [17]. Bosch et al. [18] have attributed this result to the reduction sequence:

$$\underset{+5}{V_2O_5} \rightarrow \underset{+4.33}{V_6O_{13}} \rightarrow \underset{+4}{V_2O_4} \rightarrow \underset{+3}{V_2O_3}$$

The binding energy values of the $V2p_{3/2}$ peak for the samples before TPR-H_2 are shown in Table 2. The XPS results for $V2p_{3/2}$ signal after reduction with hydrogen are presented in Fig. 5. Several authors [19–21] have calculated the average oxidation state by peaks deconvolution of the V photoelectron signal. In our case, this cannot be done, since the peak of $V2p_{3/2}$ in the V-based catalysts is very broad because of the low V-loading. The binding energy values of the V photoelectron peaks in the range 517.5–517.6, at 516.5 and at 515.9 eV are commonly attributed to respectively V^{5+}, V^{4+} and V^{3+} oxidation state of vanadium

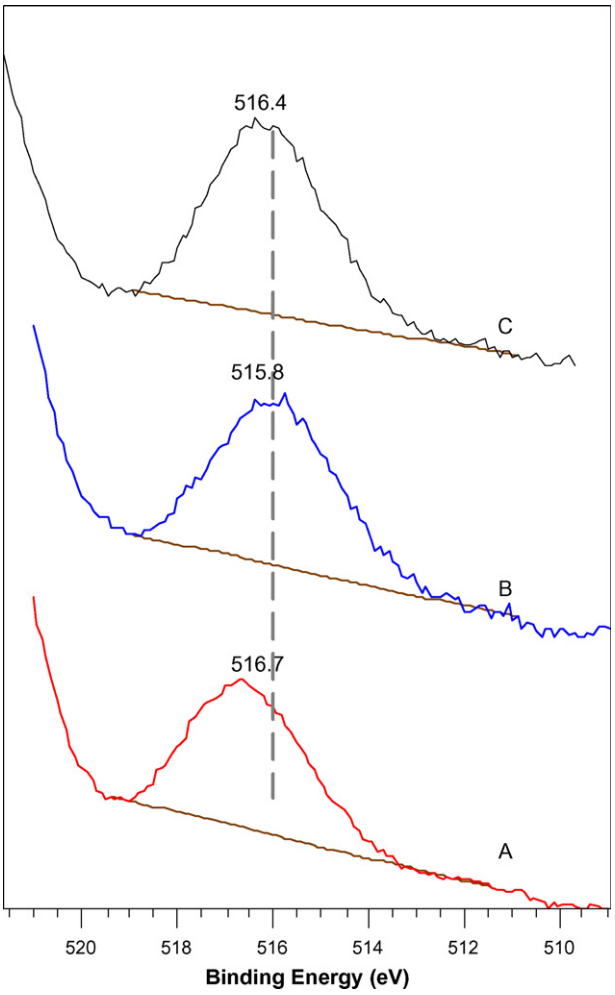

Fig. 5. XPS spectra showing the $V2_{p3/2}$ region of the (A) 5V/$AlPO_4$, (B) 5V/$Al_{0.5}Ga_{0.5}PO_4$ and (C) 5V/$GaPO_4$ after TPR-H_2.

[19]. Thus, the state of oxidation of vanadium in the samples before reduction is close to +5 (see Table 2). After TPR-H_2, on 5V/$AlPO_4$ and 5V/$GaPO_4$ the $V2p_{3/2}$ peak is centred at about 516.7 and 516.4 eV, respectively, which could be attributed to V^{4+}. However, on 5V/$Al_{0.5}Ga_{0.5}PO_4$ the $V2p_{3/2}$ peak is centred at about 515.8 eV, suggesting that the oxidation state of the vanadium on this catalyst is close to V^{3+}. Despite the deconvolution of $V2p3_{/2}$ peak cannot be done, as mentioned above, the broadness of the lines suggests the presence of vanadium in several oxidation states.

The atomic ratios for 5V/$AlPO_4$, 5V/$Al_{0.5}Ga_{0.5}PO_4$ and 5V/$GaPO_4$ fresh and after reaction are shown in Table 2. For all the spent V-based catalysts, the $P_{2p}/[(Al_{2p}) + (Ga_{3d})]$ atomic

Table 2
XPS data for V-based catalysts fresh and after catalytic test

Sample	Fresh				After test		
	$P_{2p}/[(Al_{2p}) + (Ga_{3d})]$	$V2_{p3/2}/P_{2p}$	C_{1s}/P_{2p}	$V2_{p3/2}$ (eV)	$P_{2p}/[(Al_{2p}) + (Ga_{3d})]$	$V2_{p3/2}/P_{2p}$	C_{1s}/P_{2p}
5V/$AlPO_4$	0.98	0.13	1.90	517.2	0.98	0.85	2.69
5V/$Al_{0.5}Ga_{0.5}$ PO_4	0.99	0.15	1.87	517.0	0.99	1.04	2.71
5V/$GaPO_4$	0.99	0.15	1.89	517.0	0.99	0.56	2.82

Table 3
Data for V-based catalysts and supports in propane ammoxidation

Sample	Conv. C_3H_8 (%)	Conv. NH_3 (%)	Selectivity (%)				
			ACN	AcCN	C_3H_6	C_2H_6	CO_X
$AlPO_4$	26	20.	4	33	45	4	10
$5V/AlPO_4$	49	95.	14	18	19	1	24
$Al_{0.5}Ga_{0.5}PO_4$	24	23.	5	34	35	4	10
$5V/Al_{0.5}Ga_{0.5}PO_4$	48	96	27	10	30	3	28
$GaPO_4$	20	14	7	26	44	4	11
$5V/GaPO_4$	31	81	12	29	37	2	14
SiO_2	18	21	5	24	32	10	21
$5V/SiO_2$	23	93	8	21	22	6	32

Temperature: 530 °C; feedstock: $C_3H_8/O_2/NH_3 = 1.25/3/1$, 0.1 g catalyst. ACN: acrylonitrile; AcCN: Acetonitrile.

ratio remains constant, whereas the $V2_{p3/2}/P_{2p}$ atomic ratio increases for all the catalysts. The C_{1s}/P_{2p} atomic ratio slightly increases after test whatever the catalyst, and this could be due to some coke deposition.

3.2. Catalytic activity

In a previous work [10] we have reported that, (i) the $Al_{0.5}Ga_{0.5}PO_4$ support is not selective to acrylonitrile (ACN), and (ii) the selectivity to ACN is greatly enhanced for the $5V/Al_{0.5}Ga_{0.5}PO_4$. Moreover, results obtained with a mechanical mixture ($Al_{0.5}Ga_{0.5}PO_4 + V_2O_5$) suggest that a cooperation between V_2O_5 and $Al_{0.5}Ga_{0.5}PO_4$ operates [10]. The observed products obtained during the propane ammoxidation in the presence of the catalyst were acrylonitrile (ACN), acetonitrile (AcCN), propylene, ethylene, carbon oxides (CO_x), N_2 and N_2O. The V-oxide supported catalysts showed a higher performance in propane ammoxidation at 530 °C. These results are summarized in Table 3. It can be seen that the supports present a low selectivity to nitriles products, being more selective to acetonitrile. The supports also exhibit a higher selectivity to propylene. The ethylene detected is probably formed from a parallel cracking reaction. SiO_2 is the most selective support towards ethylene production. Although an homogeneous conversion is observed, all supports show a higher conversion (Table 3) than that corresponding to homogeneous reaction. This suggests that the supports are active in propane ammoxidation.

The vanadium incorporation on the support leads to (i) an increase in the conversion of both propane and ammonia, (ii) an increase in the selectivity of acrylonitrile (ACN), (iii) a decrease in the C_3H_8, AcCN and C_2H_4 selectivities and (iv) an increase in the CO_x selectivity.

Fig. 6 shows the conversion of C_3H_8 and the selectivity to ACN at 500, 530 and 550 °C for the supports ($AlPO_4$, $Al_{0.5}Ga_{0.5}PO_4$, $GaPO_4$ and SiO_2) as well as for the V-based catalysts ($5V/AlPO_4$, $5V/Al_{0.5}Ga_{0.5}PO_4$, $5V/GaPO_4$ and $5V/SiO_2$). The propane conversion increased with the reaction

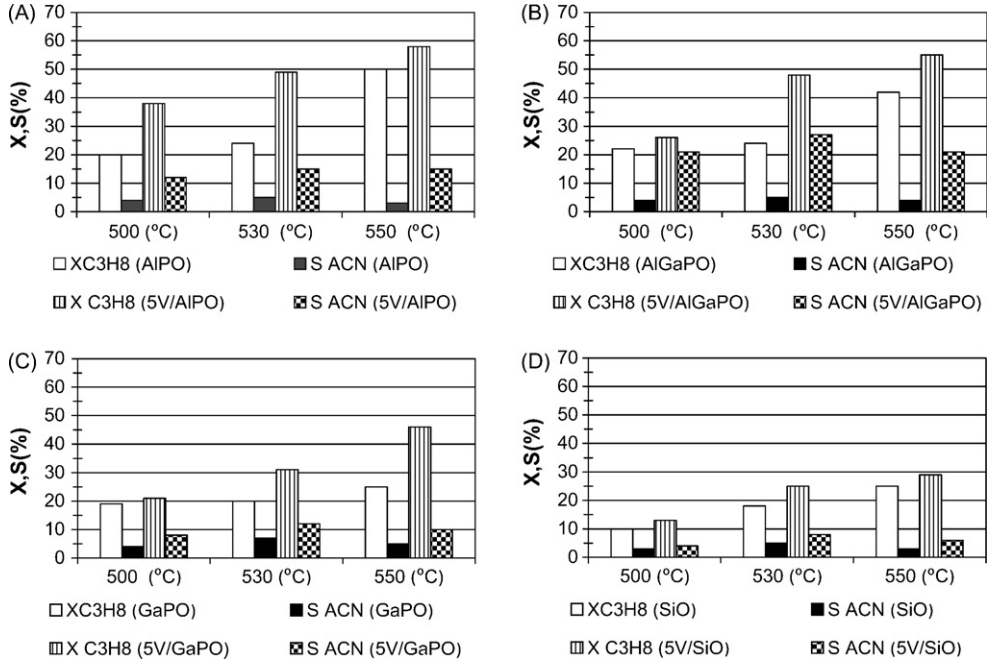

Fig. 6. Conversion of propane and selectivities as a function of the reaction temperature for (A) $AlPO_4$, (B) $Al_{0.5}Ga_{0.5}PO_4$, (C) $5V/GaPO_4$ and (D)/SiO_2, with and without V impregnated (see color code on the figures).

temperature for both supports and the V-based catalysts. The $AlPO_4$, $Al_{0.5}Ga_{0.5}PO_4$, $GaPO_4$ and SiO_2 supports are poorly selective to ACN whatever the temperature measured. Improved performances (increased conversion of the propane and selectivity to ACN) are induced by the impregnation of vanadium, regardless the nature of the support and the reaction temperature. For all V-based catalysts the selectivity to ACN reaches a maximum at 530 °C. At this temperature the selectivity to ACN increases as follows:

$$5V/Al_{0.5}Ga_{0.5}PO_4(27\%) > 5V/AlPO_4(14\%) > 5V/GaPO_4(12\%) > 5V/SiO_2(8\%)$$

However, the increase in selectivity to ACN is the highest for vanadium impregnated on $Al_{0.5}Ga_{0.5}PO_4$ while it is the lowest for $5V/SiO_2$. The latter result suggests that the higher selectivity to ACN is not due to vanadium only but is due to the simultaneous presence of V and a phosphate support.

4. Discussion

4.1. Change in the textural properties due to the impregnation of vanadium on the supports $AlPO_4$, $Al_{0.5}Ga_{0.5}PO_4$ and $GaPO_4$

As discussed previously in [10], the BET surface area of $5V/Al_{0.5}Ga_{0.5}PO_4$ decreases noticeably (79%) with respect to that of the $Al_{0.5}Ga_{0.5}PO_4$ support. In the present work, we observed the same phenomenon for the $5V/AlPO_4$ and $5V/GaPO_4$ catalysts, where a diminution of the BET surface area (76 and 90% for $5V/AlPO_4$ and $5V/GaPO_4$ respectively) was observed. It was also observed after vanadium impregnation that the total pore volume decreases by 49, 52 and 65% in $5V/AlPO_4$, $5V/Al_{0.5}Ga_{0.5}PO_4$ and $5V/GaPO_4$ respectively.

In order to discriminate if the decrease in both the BET surface area and the pore volume as well as the appearance of new pores are due to the presence of vanadium oxide and/or to an effect of the 2nd calcinations of the support when V is impregnated, the $AlPO_4$, $GaPO_4$, $Al_{0.5}Ga_{0.5}PO_4$ supports were calcined in the same conditions as the V-based samples (500 °C, 3 h). For all the calcined supports a monomodal distribution was observed, which indicates that the new pores present in V-based catalysts are due exclusively to impregnating vanadium on the supports. On the contrary, the calcination of the $AlPO_4$, $Al_{0.5}Ga_{0.5}PO_4$, $GaPO_4$, supports lead to a diminution of the BET surface area and of total pore volume. This diminution depends on the type of support. Thus, for the $AlPO_4$, $Al_{0.5}Ga_{0.5}PO_4$, $GaPO_4$ a diminution in the BET surface area of 22, 44 and 54% respectively was observed, and a diminution of 7, 30 and 30% of the total pore volume was observed.

Despite the fact that the BET surface areas for the supports decreased as a result of the calcinations, it does not explain the much more marked loss in the BET surface areas measured for the V-based catalysts. Consequently, the diminution of the BET surface area in the $5V/AlPO_4$, $5V/Al_{0.5}Ga_{0.5}PO_4$ and $5V/GaPO_4$ catalysts could be explained by two phenomena: (i) blocking of pores by V_2O_5 particles (which also produces a diminution of the total pore volume) and (ii) rearrangement in the surface during the calcination causing a partial crystallization of the support.

4.2. Crystallization of the support and the V_2O_5

XRD of V-based catalysts ($5V/AlPO_4$, $5V/Al_{0.5}Ga_{0.5}PO_4$ and $5V/GaPO_4$) showed the crystallization of the supports AlPO, $Al_{0.5}Ga_{0.5}PO_4$ and $GaPO_4$ at 500 °C. This is remarkable since the pure supports are XRD amorphous when they were calcinated at 500 °C, and need high temperatures for their crystallization: 1100 °C for $AlPO_4$, 950 °C for $Al_{0.5}Ga_{0.5}PO_4$ and 750 °C for $GaPO_4$ [12]. XRD and Raman spectroscopy also reveal the presence of crystalline V_2O_5. Similar results were previously reported by Chary et al. [22] and Lindblad et al. [23] who observed the formation of crystalline V_2O_5, as well as the crystallization of amorphous $AlPO_4$ after vanadium impregnation.

In the same way, it was shown that crystalline V_2O_5 is not responsible for the support crystallization. However, the vanadium species able to induce the crystallization of the support is a ''not yet crystallized vanadium oxide''. Actually, when the support crystallizes in presence of V, the support crystallizes first and then only the vanadium oxide.

4.3. TPR-H_2

The number of peaks in their respective TPR-H_2 experiments suggests that the reduction of V proceeds in two steps on $Al_{0.5}Ga_{0.5}PO_4$, whereas on $AlPO_4$, $GaPO_4$ and SiO_2 it occurs mainly in one step. TPR-H_2 shows that V species are reduced with a facility decreasing as:

$$5V/Al_{0.5}Ga_{0.5}PO_4(1ststep) > 5V/AlPO_4 > 5V/GaPO_4 > 5V/SiO_2.$$

XPS leads to a similar conclusion as it can be seen that, after an identical TPR-H_2 programme, the oxidation state is close to +3 for $5V/Al_{0.5}Ga_{0.5}PO_4$, whereas in the other V-based catalysts the final oxidation state of vanadium was close to +4. This different final oxidation state, which must be regarded in the line with the presence of the two TPR-H_2 peaks observed in $5V/Al_{0.5}Ga_{0.5}PO_4$ material, indicates that vanadium is reduced in a larger extent on $5V/Al_{0.5}Ga_{0.5}PO_4$ than on $5V/AlPO_4$, and $5V/GaPO_4$.

4.4. Relationship between synergy and the physicochemical properties of the V-based catalysts

The three V-based samples have specific surface areas comparably smaller than those of the supports. XRD results reveal that the presence of vanadium induced the crystallization of all the supports ($AlPO_4$, $Al_{0.5}Ga_{0.5}PO_4$ and $GaPO_4$) in similar extents. This suggests that the extent of the synergy to ACN selectivity is not due to differences in the textural or the structural properties in the catalysts.

Raman spectroscopy and XRD show the presence of crystalline V_2O_5 in the three V-based catalysts. In $5V/AlPO_4$ and $5V/GaPO_4$ catalysts, together with crystalline V_2O_5, polymeric vanadates were detected. Since the selectivity to ACN increases as follows:

$$5V/Al_{0.5}Ga_{0.5}PO_4(27\%) > 5V/AlPO_4(14\%) > 5V/GaPO_4(12\%) > 5V/SiO_2(8\%)$$

it suggests that polyvanadates are not the most selective species, and that they cannot explain entirely the highest selectivity observed for $5V/Al_{0.5}Ga_{0.5}PO_4$.

The $V2_{p3/2}/P_{2p}$ atomic ratio for spent V-based catalysts is higher than that of the fresh catalysts. These results indicate that the vanadium oxide spreads over the support, which can be responsible for the observed increase in catalytic performances. Such an increase is more marked for $5V/Al_{0.5}Ga_{0.5}PO_4$, which could explain, at least in part, the higher catalytic performance shown by this catalyst.

On the other hand, it seems that crystalline V_2O_5 plays a crucial key role in this matter. In the catalytic system NiSbV (1/2/0.3) [24] the V_2O_5 presence also was detected. This catalyst displays a certain activity in the reaction of propane ammoxidation. But in our case the activity is favoured by cooperation between the support and the V_2O_5.

As for textural and structural arguments, and for the presence the polymeric vanadates, the acidity of the V-based catalysts does not explain satisfactorily the extent of the synergy to ACN selectivity. Indeed the order of the acidity does not mach with the order of selectivity to ACN for the V-catalysts.

On the contrary, the order of selectivity to ACN coincides with the order of the reducibility of the vanadium species. The higher facility of V_2O_5 reduction on $Al_{0.5}Ga_{0.5}PO_4$ could thus explain in a convincing way the higher selectivity to ACN obtained in the $5V/Al_{0.5}Ga_{0.5}PO_4$ catalyst.One has to admit that, at this stage, the hypothesis should still be experimentally supported. However, by analogy with other similar systems (Mo oxide catalysts or VPO oxide catalysts used in oxidation reaction), the idea that catalysts containing a small amount of reduced metal with fully oxidized metal are more selective, could be a reasonable one [25,26].

5. Conclusions

Catalytic performances are boosted by the presence of crystalline V_2O_5 formed on (Al)(Ga)PO supports. The extent of the synergy is not related to any variation of acidity, texture or structure neither to the presence of polymeric vanadates. But the extent of the synergy seems related to the extent of the facilitation of the reduction of V_2O_5. $Al_{0.5}Ga_{0.5}PO_4$ nonetheless offers the easiest reduction of V_2O_5 but also offers a certain tunability of the reduced species stabilized. Although the origin of the best performance of these V reduced species should still be experimentally evidenced, one assumes that this combination explains the best performance of $5V/Al_{0.5}Ga_{0.5}PO_4$ in propane ammoxidation.

Acknowledgements

The authors gratefully acknowledge the ''Fonds Spécial de la Recherche'' (FSR) for the financial support. The involvement of Unité de catalyse et de chimie des matériaux divisés in the ''CONCORDE'' Coordinated Action and in the ''FAME'' Network of Excellence of the EU 6th FP, as well as in the ''Supramolecularity'' IUAP network sustained by the ''Service public fédéral de programmation politique scientifique'' (Belgium), is acknowledged.

References

[1] G. Centi, R.K. Grasselli, F. Trifiro, Catal. Today 13 (1992) 661.
[2] G. Centi, S. Perathoner, F. Trifiro, Appl. Catal. A 157 (1997) 143.
[3] S. Albonetti, G. Blanchard, P. Burattin, T.J. Cassidy, S. Masetti, F. Trifiro, Catal. Lett. 45 (1997) 119.
[4] M. Baca, A. Pigamo, J.L. Dubois, J.M.M. Millet, Top. Catal. 23 (2003) 39.
[5] R.K. Grasselli, D.J. Buttrey, J.P. DeSanto, J.D. Burrington, C.G. Lugmair, J.A.F. Volpe, T. Weingand, Catal. Today 91 (2004) 251.
[6] G. Centi, T. Tosarelli, F. Trifiro, J. Catal. 142 (1993) 70.
[7] G. Centi, S. Perathoner, J. Catal. 142 (1993) 84.
[8] R. Prada Silvy, M. Florea, N. Blangenois, P. Grange, AIChE J. 49 (2003) 2228.
[9] M. Florea, R. Prada-Silvy, P. Grange, Catal. Lett. 87 (2003) 63.
[10] M.A. Soria, S. Delsarte, E.M. Gaigneaux, P. Ruiz, Appl. Catal. A 325 (2007) 296.
[11] K. Kearby, in: Proceedings of the 2nd International Congress Catalyst, 1961, p. 2567.
[12] V. Peltier, R. Conanec, R. Marchand, Y. Laurent, S. Delsarte, E. Gueguen, P. Grange, Mater. Sci. Eng. B47 (1997) 177.
[13] S. Brunauer, P.H. Emmet, J. Am. Chem. Soc. 60 (1938) 309.
[14] E.P. Barret, L.G. Joiyner, P.P. Halenda, J. Am. Chem. Soc. 73 (1953) 373.
[15] J.M. Kanervo, M.E. Harlin, A.O.I. Krause, M.A. Bañares, Catal. Today 209 (2002) 43.
[16] J.-M. Jehng, J. Phys. Chem. B 102 (1998) 5816.
[17] M.M. Koranne, J.G. Goodwin Jr., G. Marcelin, J. Catal. 148 (1994) 369.
[18] H. Bosch, B.J. Kip, J.G. Van Ommen, P.J. Gelling, J. Chem. Soc. 80 (1984) 2479.
[19] M.E. Harlin, V.M. Niemi, A.O.I. Krause, J. Catal. 195 (2000) 67.
[20] B.M. Weckhuysen, D.E. Keller, Catal. Today 78 (2003) 25.
[21] B.P. Barbero, L.E. Cadus, Appl. Catal. 272 (2004) 69.
[22] K.V.R. Chary, G. Kishan, K. Ramesh, Ch.P. Kumur, G. Vidyasagar, Langmuir 19 (2003) 4548.
[23] T. Lindblad, B. Rebenstorf, Z.-G. Yan, S.L.T. Andersson, Appl Catal. A 112 (1994) 187.
[24] T.J. Cassidy, M. Pollastri, F. Trifiro, J. Catal. 172 (1997) 55.
[25] E.M. Gaigneaux, M.J. Genet, P. Ruiz, B. Delmon, J. Phys. Chem. B 104 (2000) 5724.
[26] K. Aït-Lachgar, M. Abon, J.C. Volta, J. Catal. 171 (1997) 383.